A&A 413, L1–L4 (2004)
DOI: 10.1051/0004-6361:20034621

Astronomy & Astrophysics

Near infrared imaging of NGC 2316⋆

P. S. Teixeira[1], S. R. Fernandes[1], J. F. Alves[2], J. C. Correia[1], F. D. Santos[1], E. A. Lada[3], and C. J. Lada[4]

[1] Depart. de Física, Faculdade de Ciências da Universidade de Lisboa, Ed. C8, Campo Grande, 1749-016 Lisboa, Portugal
e-mail: psteixeira@fc.ul.pt; srfernandes@fc.ul.pt; jcc@fc.ul.pt; fdsantos@fc.ul.pt
[2] European Southern Observatory, ESO, Germany
e-mail: jalves@eso.org
[3] Department of Astronomy, University of Florida, USA
e-mail: lada@astro.ufl.edu
[4] Harvard-Smithsonian Center for Astrophysics, CfA, USA
e-mail: clada@cfa.harvard.edu

Received 16 July 2003 / Accepted 15 November 2003

Abstract. In the present paper we present *JHK* photometric results of the young embedded cluster NGC 2316. We construct the cluster radial profile from which we determine a radius of 0.63 pc. We find 189 ± 29 cluster members in an extinction limited sub-sample of the survey, 22 ± 19 of which are possibly substellar. An average extinction of 4.5 visual magnitudes is derived using $(H - K)$ colours of control fields. This extinction is due to the presence of residual parental molecular cloud. NGC 2316 presents 16% source fraction of excess emission which is consistent with other results from clusters with an age of 2–3 Myr. This age is consistent with the distribution of sources in the colour-magnitude diagram when compared to theoretical isochrones, and the overall shape of the cluster KLF. The substellar population of the cluster is similar or smaller than that observed for other embedded clusters and the stellar objects dominate the cluster membership.

Key words. stars: formation – stars: low-mass, brown dwarfs – stars: planetary systems: protoplanetary disks – stars: luminosity function – infrared: stars – ISM: individual objects: NGC 2316

1. Introduction

Embedded clusters may be the fundamental units of star formation (Lada & Lada 2003). They contain statistically significant samples of young stars of similar age and composition spanning a wide range of mass, providing excellent laboratories for investigating a number of important issues in star formation such as the form and universality of the initial mass function (IMF) and the frequency and lifetimes of protoplanetary disks. Surveys for near infrared (NIR) excess in embedded clusters can provide knowledge of the disk frequency and evolution because a protoplanetary disk is easier to detect than a planetary system with a similar mass of solid material (Beckwith & Sargent 1996). In addition, embedded clusters provide the smallest spatial scale for investigating the nature of the IMF, its form and universality; their mass function is in fact an initial mass function since young clusters have not lost significant numbers of members to either dynamical or stellar evolution.

NGC 2316 is a young partially embedded cluster with coordinates $(\alpha, \delta)(J2000) = (6^h59^m40^s, -7°46'36'')$ at a distance of 1.1 kpc according to Felli et al. (1992) and Hodapp (1994). There is an HII region centered on a B3 ZAMS star (Noguchi et al. 1993; Fukui et al. 1993), associated with the IRAS 06572−0742 source. The UV radiation is apparently creating a dense photodissociated region (Ryder et al. 1998), showing some physical signatures of ongoing star formation, such as H_2O masers (Felli et al. 1992) and CO outflow with spectral index characteristic of optically thin free-free emission (Beltrán et al. 2001). NGC 2316 was first uncovered by Parsamian (1965), followed by other studies (e.g. Hodapp 1994), however certain parameters are still not well established. To better characterize this cluster we obtained deep multi wavelength NIR images of the region to better constrain the cluster's age and spatial distribution, as well as provide estimates of membership number, fraction of NIR excess sources and brown dwarf population.

2. Observations

The observations were made on the 8th and 9th of March 1999 using the SofI infrared camera (J (1.25 μm), H (1.65 μm), and Ks (2.162 μm) bands) on the 3.5 m NTT telescope in La Silla, Chile. We took 45 images per band, with a total integration time of 900 s. Two control fields were taken also in

Send offprint requests to: P. S. Teixeira,
e-mail: psteixeira@fc.ul.pt

⋆ Based on observations carried out at ESO, La Silla, Chile.

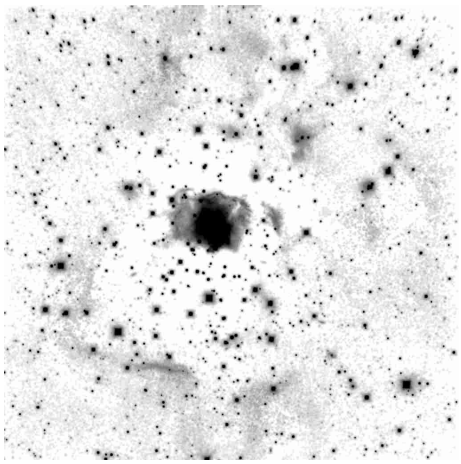

Fig. 1. NGC 2316 *JHK*s combined grey scale image from the NTT data. The scale is stretched to enhance the low level emission due to residual cloud material. The large majority of sources in this image are not visible at optical wavelengths. The field size is $5' \times 5'$.

*JHK*s bands, one located 20′ N of the NGC 2316's center, the other located 13′ S, with a total integration time of 90 s. The field of view was aproximately $5' \times 5'$, with a pixel scale of 0.29″ per pixel. The average FWHM of point sources in the final image is about 0.54″. In Fig. 1 we can observe that NGC 2316 presents a residual cloud material, nicely visible as a bubble centered on the cluster's core. This faint nebulae, surrounding the B star in the center of the cluster, is indicative of the early age of this cluster, less than 5 Myr when compared to NGC 2362 (Moitinho et al. 2001) which shows no nebulosity.

3. Data analysis

The data reduction for NGC 2316 cluster is done using the IRAF[1] DIMSUM (Deep Infrared Mosaicing Software) package, to reconstruct dithered exposures taken for *J*, *H* and *K*s filters. Astrometry is conducted with ESO's (European Southern Observatory) SKYCAT tool and the IRAF routines IMTRANSPOSE, CCMAP and CCSETWCS. Infrared sources are identified using SExtractor (Bertin & Arnouts 1996) and checked through visual inspection. A FWHM of 0.5″ is used, along with a Gaussian filter of 3 sigma, a detection threshold of 3 sigma and a deblending threshold parameter of 64 with a minimum contrast of 0.0005 counts. We use the SExtractor output to remove approximately 80 galaxies from the cluster and control fields *K*–band data. Photometry is done with the routine PHOT of the IRAF's PHOTCAL package, using an aperture radius of 5 pixels (0.73″) for the cluster and 6 pixels (0.87″) for the two control fields with appropriate aperture corrections per band. Finally, for the photometric calibration we reduced 9 exposures of the standard star 9118 from the Persson catalog (Persson et al. 1998), determining the zero point by using the filter transformation equations in the SofI's camera web page[2].

[1] *Image Reduction and Analysis Facility* (IRAF) is distributed by NOAO, which is operated by AURA, Inc., under contract to the NSF.

[2] `http://www.ls.eso.org/lasilla/Telescopes/NEWNTT/sofi/`

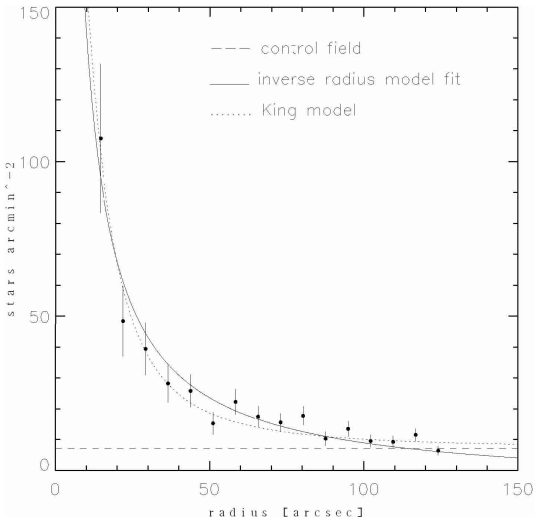

Fig. 2. *K*-band radial profile of NGC 2316. The error bars represent the $\sqrt{N}$ statistical error in each bin. The dashed line corresponds to the background density determined from averaging the reddened ($\langle A_V \rangle$ = 4.5 mag) control field. Two fits are plotted, one using the King (1962) model, the other an inverse radius profile. From this we estimate the cluster radius to be 120″, or 0.63 pc.

We converted our *K*s photometric results to *K* fotometry using these equations to better compare with other similar studies on young clusters. Comparing our photometry with 2MASS photometry[3], we find an average difference in *J*, *H* and *K* magnitudes of 0.04, 0.02 and 0.04, respectively and an average difference in $(H - K)$ colours of −0.01 and in $(J - H)$ of 0.03, so no further calibration is needed.

4. Results

In the present *JHK* photometry survey of NGC 2316, we detected 1067 sources at *J*–band, 1229 sources at *H*–band, and 1251 sources at *K*–band. The completeness limits of the observations are 18.0, 18.5 and 20.0 for the *K*, *H*, and *J*–bands, respectively, in the cluster field, and 17.5, 17.5, 18.0 for an averaged control field. These are estimated from the luminosity functions, where we consider our sample complete up to the bin imediately before the maximum. For the data analysis the control field completeness limits were used and no extrapolation was made to account for sensitivity diferences between the two fields observed.

4.1. Radial profile

Figure 2 presents the *K* radial density profile, where only the sources brighter than the completeness limit were included. The profile is centered on the peak of the stellar density distribution. NGC 2316 presents a regular distribution falling steeply

[3] This publication makes use of data products from the Two Micron All Sky Survey, which is a joint project of the University of Massachusetts and the Infrared Processing and Analysis Center/California Institute of Tecnology, funded by the National Aeronautics and Space Administration and the National Science Foundation.

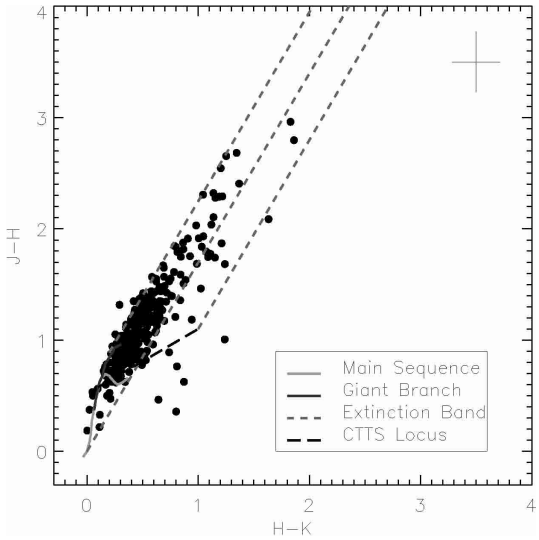

Fig. 3. $(H - K)$ vs. $(J - H)$ colour-colour diagram for NGC 2316 sources. The giant branch and main sequence from Bessell & Brett (1988) are shown, along with the Classical T Tauri locus from Meyer et al. (1997). The reddening vector was determined using the values of extinction from Rieke & Lebofsky (1985). Photometric errors are illustrated at the upper right.

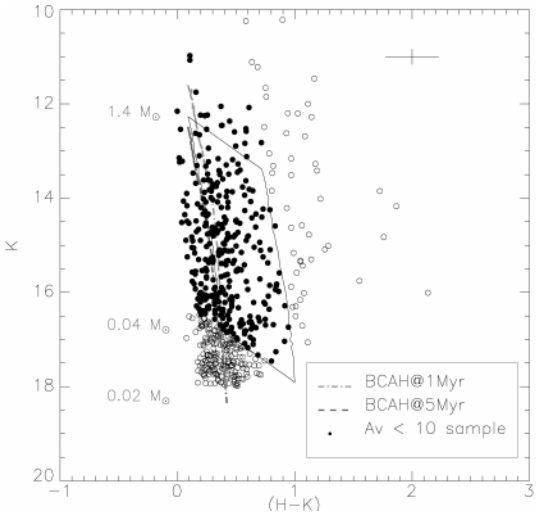

Fig. 4. K vs. $(H - K)$ colour-magnitude diagram for the entire survey. The data are compared with the 1 and 5 Myr isochrones of Baraffe et al. (1998) at a distance of 1.1 kpc. A sample is selected for sources with $A_V < 10$; the reddening slope is determined from Rieke & Lebofsky (1985).

and merging with the extincted background at 120″ (0.63 pc). The stellar surface density distribution exhibits more of a centrally condensed and relaxed structure than a hierarchical type structure (e.g., Lada & Lada 2003). Within the 120″ radius, the number of cluster members is 158 ± 20. Assuming a spherical geometry and an average mass per star of $0.3\,M_{\odot}$, we determine the stellar volume density to be $45\,M_{\odot}\,\mathrm{pc}^{-3}$. Two models are fitted to our radial profile as shown in the figure. The King model (King 1962) is given by the expression $n(r) = f_0/[1 + (r/r_c)^2]$, where f_0 is the core concentration at zero radius and r_c is the core radius. This function agrees sufficiently with our data ($\chi^2 = 0.81$) to provide an estimate of the core radius and density. The parameters are determined to be 300 stars arcmin^{-2} ($72\ M_{\odot}\,\mathrm{pc}^{-3}$) and 10″ (0.05 pc) respectively for f_0 and r_c. An inverse radius model ($n(r) = -5.77 + 1466.61/r$, $\chi^2 = 0.94$) also describes fairly well the density distribution. We also note some oscilations in the density distribution that can be of statistical origin.

4.2. Colour-colour diagram

The infrared *JHK* colour-colour diagram of NGC 2316 is plotted in Fig. 3, considering only sources brighter than the completeness limits for each band and located inside the cluster radius, as determined in the previous section. There is a considerable spread of stars along the reddening band, which corroborates with the previous statement that the cluster is partially embedded. $(J - H)$ and $(H - K)$ colours are also calculated for the two control fields for comparison. The latter fields show almost no reddening. Subtracting this contamination we find 16% ± 3% of cluster members with NIR excess emission characteristic of young stars with circumstellar disks (Lada & Adams 1992).

4.3. Colour-magnitude diagram

The infrared colour-magnitude diagram for NGC 2316 is presented in Fig. 4 for sources with magnitudes above the completeness limits. We compare source locations with the theoretical isochrones of 1 and 5 Myrs from the Baraffe et al. (1998) non-grey evolutionary models at a distance of 1.1 kpc (Felli et al. 1992). There is some spread of sources to the left of the isochrones due to foreground contamination. From the diagram, we observe a much wider spread of sources to the right of the isochrones, a result of extinction produced by the associated molecular cloud. In order to derive the cluster KLF, we construct a statistically more complete mass and extinction sample by including only objects with $A_V < 10$ mag and mass $>0.04\,M_{\odot}$, for which we are essentially complete. This diagram is not a good discriminant for the cluster age so we assume an intermediate age of 3 Myrs for the construction of our mass limited and extinction limited sample.Within the errors this sample is also valid for cluster ages of 1−5 Myr.

4.4. Luminosity function

The absolute K luminosity function of the cluster (KLF), adjusted for extinction, is plotted in Fig. 5, where the hydrogen burning limit is indicated by a vertical line. Here we only use sources from the sample determined from the colour-magnitude diagram. This KLF is determined by subtracting a reddened control field from the original reddened on field. The off fields are averaged into a final control field and scaled so that the control field and the on field have both the same area. The extinction is determined from the average colour excess of the NGC 2316 field as compared to the control field ($\Delta(H - K) = \langle(H - K)_{\mathrm{cluster}}\rangle - \langle(H - K)_{\mathrm{controlfield}}\rangle$) using sources with no NIR excess emission. This average colour excess is used to determine the extinction following the Rieke & Lebofsky (1985) law and is found to be

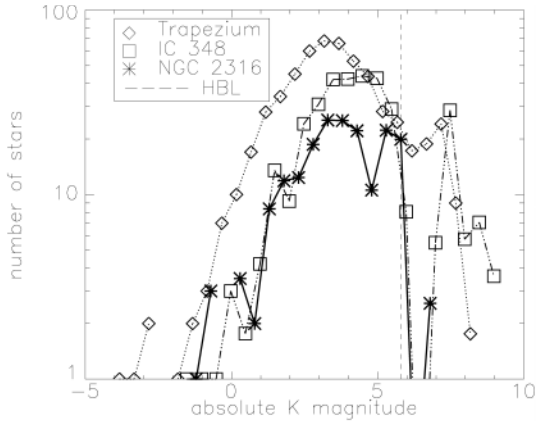

Fig. 5. Dereddened KLF of NGC2316, compared to the KLFs of the Trapezium and IC 348 clusters. The vertical dotted line indicates the hydrogen burning limit (HBL), (Baraffe et al. 1998) for NGC 2316 assuming a distance of 1.1 kpc and an age of 3 Myr.

$\langle A_V \rangle$ = 4.5 mag with a standard deviation of approximately 5 mag. We compare this luminosity function with those of Trapezium (Muench et al. 2002) and IC 348 (Lada & Lada 1995), where we find a striking similarity between the shapes of NGC 2316 and IC 348 KLFs. We estimate a membership of 189 ± 29 and a number of objects beyond the HBL of 22 ± 19. This is a very crude estimate because although we are sensitive to masses as low as 20 $M_{\rm Jup}$, the background contamination dominates the statistical errors for the substellar KLF bins at NGC 2316's distance.

5. Discussion and summary

Circumstellar disks emit at NIR wavelengths. Studying the NIR excess emission of young cluster sources provides thus information on the frequency of circumstellar disks. Our estimate of the NIR excess emission for NGC 2316 according to the colour-colour diagram is 16% ± 3%.

We conclude that NGC 2316's members span a wide range of masses, from B–stars down to the substellar regime (40 $M_{\rm Jup}$), and is significantly embedded ($\langle A_V \rangle$ = 4.5) in its parental molecular cloud. We estimate a size of 0.63 pc for NGC 2316 from the radial profile assuming a distance of 1.1 kpc. Using an extinction limited sub-sample of the survey, we derive a membership for the entire cluster of 189 ± 29 objects, of which 22 ± 19 are beyond the HBL.

Regarding the crude estimate of the substellar population we note that studies of clusters at distances around and beyond 1 kpc will be hampered by an overwhelming background contamination at the faintest magnitudes (that cannot be reduced by deeper observations). Nevertheless, the estimated fraction of substellar objects in NGC 2316 (2−22%) is comparable, within the errors, to that derived for the Trapezium cluster (20−25% Muench et al. 2002) and IC 348 (14−20% Muench et al. 2003) from a similar KLF analysis. This is additional evidence that brown dwarfs do not make a significant contribution to the overall cluster, either by numbers or mass. In other words, the population of these clusters is dominated by stellar rather than substellar members.

The NIR excess emission obtained for NGC 2316 from *JHK* photometry is likely an underestimate. Significant emission of a circumstellar disk is in the *L*–band (3.4 μm), arising from warm circumstellar material within a few stellar radii, so *JHKL* photometry would provide a more complete census of excesses, (Liu et al. 2003). IC 348, a cluster of approximately 3 Myr, presents a fraction of NIR excess sources of 21% using *JHK* photometry and 65% using *JHKL* photometry, (Haisch et al. 2001; Lada et al. 2000). On the other hand, NGC 2316 has a bright UV source, a central B3 star, which might accelerate the dissipation of circumstellar disks by photoevaporation and consequently decrease the number of observed sources with NIR excesses.

The comparison of the NGC 2316, IC 348 and Trapezium KLFs in Sect. 4.4 shows good agreement between their shapes; in particular, the first two are very similar (apart from the number of sources), as they roughly show the same broad peak at the same absolute magnitudes. Assuming an universal IMF, (e.g. Lada & Lada 2003), we infer that NGC 2316 has approximately the same age as IC 348, about 2–3 Myr (Lada & Lada 1995; Muench et al. 2003), but is more evolved and older than the Trapezium.

Acknowledgements. We thank Lynne Hillenbrand for helpful discussion. This research is financially supported by Fundação para a Ciência e Tecnologia (FCT), Portugal, under the project *PESO/P/PRO/40154/2000*. J. C. Correia gratefully acknowledges the financial support from FCT through the grant *SFRH/BPD/3614/2000*.

References

Baraffe, I., Chabrier, G., Allard, F., & Hauschildt, P. H. 1998, A&A, 337, 403
Beckwith, S. V. W., & Sargent, A. I. 1996, Nature, 383, 139
Beltrán, M. T., Estalella, R., Anglada, G., Rodríguez, L., & Torrelles, J. M. 2001, AJ, 121, 1556
Bertin, E., & Arnouts, S. 1996, A&AS, 117, 393
Bessell, M. S., & Brett, J. M. 1988, PASP, 100, 1134
Felli, M., Palagi, F., & Tofani, G. 1992, A&A, 255, 293
Fukui, Y., Iwata, T., Mizano, A., Bally, J., & Lane, A. P. 1993, Protostars and Planets III, 603
King, I. 1962, AJ, 67, 471
Haisch, K. E. Jr., Lada, E. A., & Lada, C. J. 2001, AJ, 121, 2065
Hodapp, K. W. 1994, ApJS, 94, 615
Lada, C. J., & Adams, F. C. 1992, ApJ, 393, 278
Lada, C. J., Muench, A. J., Haisch, K. E. Jr., et al. 2000, AJ, 120, 3162
Lada, C. J., & Lada, E. A. 2003, ARA&A, in press
Lada, E. A., & Lada, C. J. 1995, AJ, 109, 1682
Liu, M., Najita, J., Tokunaga, A., & Alan, T. 2003, ApJ, 585, 372
Meyer, M. R., Calvet, N., & Hillenbrand, L. A. 1997, AJ, 114, 288
Moitinho, A., Alves, A., Huélamo, N., & Lada, C. 2001, ApJ, 563, 73
Muench, A. A., Lada, E. A., Lada, C. J., & Alves, J. F. 2002, AJ, 573, 366
Muench, A. A., Lada, E. A., Lada, C. J., et al. 2003, AJ, 125, 2029
Noguchi, K., Qian, Z., Wang, G., & Wang, J. 1993, PASJ, 45, 65
Parsamian, E. S. 1965, Izv. Akad. Nauk. Armyan. SSR., Ser. Fiz.-Math, 18, 146
Persson, S. E., Murphy, D. C., Krzeminski, W., Roth, M., & Rieke, M. J. 1998, AJ, 116, 2475
Rieke, M. J., & Lebofsky, L. A. 1985, ApJ, 288, 618
Ryder, S. D., Allen, L. E., Burton, M. G., Ashley, M. C. B., & Storey, J. W. V. 1998, MNRAS, 294, 338